Preprints of the 21st IFAC World Congress (Virtual)
Berlin, Germany, July 12-17, 2020

Adaptive and Robust Control for Energy Efficiency Enhancement of a Solar-powered Desalination System ⋆

Mohammad Alharbi * **Fahad Aljehani** * **Ibrahima N'Doye** *
Taous-Meriem Laleg-Kirati *

* *Computer, Electrical and Mathematical Sciences and Engineering Division (CEMSE), King Abdullah University of Science and Technology (KAUST), Thuwal 23955-6900, Saudi Arabia (e-mail: mohammad.alharbi@kaust.edu.sa, fahad.aljehani@kaust.edu.sa, ibrahima.ndoye@kaust.edu.sa, taousmeriem.laleg@kaust.edu.sa)*

Abstract: In this paper, an adaptive control strategy is proposed to enhance the energy production efficiency under environmental changes. The control objective is to force the outlet temperature of a solar thermal collector fluid to track the desired reference temperature regardless of the solar irradiance variations. An adaptive nonlinear control that combines an inner loop feedback control and an outer loop model-free control strategy is proposed to ensure asymptotic convergence of the tracking error. The proposed adaptive control strategy is applied to an approximate bilinear model derived from the heat transfer equation. Numerical simulations are presented to illustrate the performance of the control strategy in terms of tracking accuracy and settling time. Furthermore, the improvement in energy production is highlighted through a powering thermal membrane distillation based desalination in increasing water production.

Keywords: Parabolic solar collector plant, water desalination system, bilinear approximate model, model-free control, adaptive feedback controller.

1. INTRODUCTION

Nowadays, renewable energy significantly attracts the public and private sectors toward more sustainable energy production. Moreover, the exponential growth of the energy demand is accompanied with a decrease in fossil resources along with an accelerating environmental overuse and destruction requiring sustainable alternative energy resources. One of the promising clean source of energy is the solar energy with the huge amount of received sunlight which could sustain the world energy demand. Continuous investigations in solar thermal systems showed that the areas of improvement are in the design and control to increase the efficiency of energy production. Control of the thermal distributed concentrated solar collector is one of the highly addressed topics in area of improving the energy production. Different applications benefit from the thermal energy produced by the solar collector.

An example of such a hybrid system is the solar driven membrane distillation used for water desalination. It is known that water desalination provides an alternative solution to potable water supply in some countries to meet the increasing water demand. However, conventional water desalination systems are costly and energy inefficient. Therefore there is a desire to develop new sustainable desalination systems. Membrane distillation technology is a suitable candidate for such sustainable desalination systems as it consists of feed sea water container and a cold potable water container that are separated by a hydrophobic membrane. The sea water can be directly heated with a solar systems such as the parabolic solar collector Karam and Laleg-Kirati (2016); Gálvez et al. (2009); Bendevis et al. (2019). The later consists of a parabolic shaped mirror to focus the sunlight into a central tube to heat the fluid passing through this tube where the thermal energy is produced. The system is subject to different external disturbances such as variations of the solar irradiance, the partial shading of the collectors, the annual pluvial cycles, the humidity levels, and dust accumulation. Therefore, advanced control design is required to reject and cope with these external disturbances.

Control design in the concentrated distributed solar collector can be used to enhance the production of the thermal energy. There are some basic control approaches that have been proposed such as proportional-integral-derivative control and feedforward control Camacho et al. (2007b). These controllers consider an approximated model that can be seen as a black-box or semi-discrete model. Some other studies developed other controllers based on the distributed model Rorres et al. (1980); Orbach et al. (1981); Carotenuto et al. (2007); Silva et al. (2003b); Johansen and Storaa (2002). In addition, the thermal efficiency can be improved by reducing the energy loss in a short time. This can be achieved by using control strategies and study the performance of the reference tracking and transient response. Furthermore, the effect of unpredictable work-

⋆ This work has been supported by the King Abdullah University of Science and Technology (KAUST), Base Research Fund (BAS/1/1627-01-01) to Taous Meriem Laleg.

ing conditions can be reduced when adaptive and robust control techniques are used.

The indicator for a good designed control is to reduce the intermittency problem of the solar irradiation. Doing so will result in efficient and better functioning of the control systems. A solution to that is to use the source term estimation value to update the controller and that will compensate for the external disturbances. Moreover, several control strategies combined with identification or estimation methodologies have been proposed such as the model predictive control in Gallego and Camacho (2012); Camacho and Berenguel (1997), the indirect adaptive control in Camacho et al. (1992); Igreja et al. (2014), the adaptive fuzzy switching control techniques in Henriques et al. (1999), or advanced control techniques in Camacho et al. (1997, 2007a); Silva et al. (2003a); Pin et al. (2008). Feedforward control is shown to be efficient and minimize the effect of disturbances in Cirre et al. (2007). Implementing a feedforward controller requires dependable measurements of the external perturbations. However, some parameters are expensive or technically hard to measure. For instance, the solar irradiance can be measured only locally using pyheliometers and reflectometers. In addition, it is not easy to obtain appropriate metal tubes absorptance estimation. An adaptive control law is a better choice in term of control systems' efficiency because it is able to adjust to variation of the system parameters.

In the hybrid solar driven membrane distillation systems, the problem can be investigated within different aspects. Recently, optimal control strategies have been proposed on the desalination part to enhance the water production Guo et al. (2019); Bendevis et al. (2019). In this paper, an enhanced adaptive controller is introduced by adding an integral term on the control design described in Elmetennani and Laleg-Kirati (2017). The new proposed adaptive control scheme helps to improve the tracking performance and the transient response within competitive times. In addition, asymptotic convergence of the global system is achieved. Furthermore, the performance of the proposed control algorithm ensures excellent tracking of the reference level which present a great impact when it is used for powering thermal dependant plants like direct contact membrane distillation (DCMD).

This paper is organized as follows. Section 2 describes the coupled solar thermal collector and membrane distillation plant, where a reduced order model of the concentrated solar collector derived from the distributed heat transport equation. Section 3 proposes the inner loop feedback control and the outer loop based model-free control. Section 4 illustrates and discusses the obtained results with numerical tests. Finally, section 5 presents some concluding remarks.

2. PROBLEM FORMULATION

The objective is to improve the water production by powering the membrane distillation process from solar collector. Fig. 1 shows the diagram of the coupled system (solar thermal collector and membrane distillation). Although, the membrane distillation process requires a steady inlet feed temperature which is not easy to obtain from thermal solar collector due to the external environmental changes.

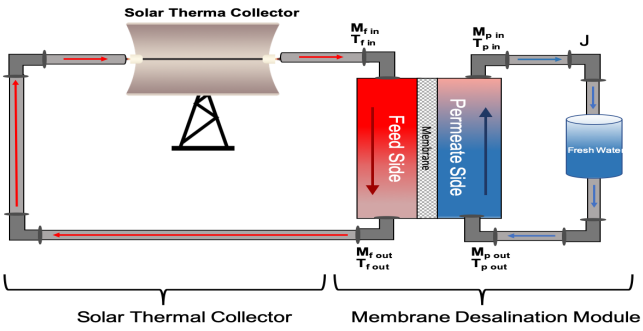

Fig. 1. Solar-powered membrane distillation plant

To deal with this issue, a bilinear approximate model has been used with the proposed control strategy to enhance the tracking performance of the parabolic solar collector which result in improving the water production.

The concentrated parabolic distributed solar collector system consists of a parabolic shaped mirror that concentrates solar irradiance on a central pipe which contains a heat thermal carrier for generation of thermal energy. The central pipe is the one that receives the heat from the sunlight. Then, the water will be heated by passing through the parabolic mirror. At the end of the pipe is where the outlet temperature is measured. Then, the heated water from the solar collector passes through the feed side of membrane distillation process. Meanwhile, cooler temperature passes through permeate side. This process leads to a pressure difference between the two sides of the membrane. The pressure difference moves the evaporated water from the feed side to the permeate side.

2.1 Distributed Solar Collector Model

The heat transfer dynamics between the thermal carrier and the collector is represented by a first-order hyperbolic PDE. It has been obtained by neglecting the heat losses and the thermal exchange between the collector tube and the thermal carrier fluid Camacho et al. (1997, 2007b); Silva et al. (2003b,a); Johansen and Storaa (2002); Farkas and Vajk (2002); João et al. (2014). This model conserves the distributed dynamics of the system for reasonable control design. The dynamics of the heat transfer along the tube is given by

$$\begin{cases} T_t(x,t) + u(t)T_x(x,t) = s(t),\ x \in (0,L],\ t \in \mathbb{R}^+ \\ T(0,t) = T_{in}(t), \quad t \in \mathbb{R}^+, \\ T(L,t) = T_{out}(t) = y(t), \quad t \in \mathbb{R}^+, \end{cases} \tag{1}$$

such that $T_x(x,t) \equiv \frac{\partial T(x,t)}{\partial x}$ and $T_t(x,t) \equiv \frac{\partial T(x,t)}{\partial t}$ are the first derivatives with respect to space and time, respectively. $T(x,t)$ is the thermal carrier fluid which represents the heat transfer phenomena in the collector tube. The source term is defined by $s(t) = \frac{\nu G}{\rho c A_s} I(t)$ whereas $s(t)$ depends on the solar irradiance $I(t)$. The fluid velocity is defined by $u(t) = \frac{Q(t)}{A_s}$ whereas $u(t)$ depends on the flow rate $Q(t)$. The system parameters of the solar collector field are summarized in Table 1.

2.2 Bilinear Approximate Model

Inspired by Elmetennani and Laleg-Kirati (2016, 2017) work, an approximate model based on radial Gaussian

Table 1. Solar Collector Field Parameters Camacho et al. (1997)

Symbol	Unit	Description
t	s	Time
x	m	space
$T(x,t)$	°C	temperature
$Q(t)$	$\mathrm{m^3\,s^{-1}}$	Fluid flow rate
ρ	$\mathrm{kg\,m^{-3}}$	Fluid density
c	$\mathrm{J\,°C^{-1}\,kg^{-1}}$	Fluid specific heat capacity
A_s	$\mathrm{m^2}$	Cross-sectional area
ν		Mirror optical efficiency
G	m	Mirror optical aperture
$I(t)$	$\mathrm{W\,m^{-2}}$	Solar irradiance
L	m	Tube length

functions of the first-order hyperbolic distributed model (1) using a low dimensional bilinear state space representation. The original method of Elmetennani and Laleg-Kirati (2016, 2017) is explained in this part for proper understanding of the improvement and changes proposed in the present paper. A brief summary of the works of Elmetennani and Laleg-Kirati (2016, 2017) is presented. The approximate temperature $T(x,t)$ is expressed as follows

$$T(x,t) \approx \hat{T}(x,t) = \sum_{i=1}^{n} \xi_i(t)\gamma_i(x), \tag{2}$$

where the basis functions $\gamma_i(x)$ is radial Gaussian functions and $\xi_i(t)$ are temporal weighting functions. After substituting $\hat{T}(x,t)$ in (1) then uniformly discretize the system using p knots and Δx as spacing distance on the domain $[0, L]$ we obtain

$$\Gamma\dot{\xi}(t) + \Gamma_x \xi(t)u(t) = S(t), \quad \text{such that} \tag{3}$$

$$\Gamma = \begin{bmatrix} \gamma_1(0) & \cdots & \gamma_n(0) \\ \gamma_1(\Delta x) & \cdots & \gamma_n(\Delta x) \\ \vdots & & \vdots \\ \gamma_1(j) & \cdots & \gamma_n(j) \\ \vdots & & \vdots \\ \gamma_1(L) & \cdots & \gamma_n(L) \end{bmatrix}_{p\times n}, S(t) = \begin{bmatrix} s(0,t) \\ \vdots \\ s(j,t) \\ s(j+\Delta x,t) \\ \vdots \\ s(L,t) \end{bmatrix}_{p\times 1},$$

$$\Gamma_x = \begin{bmatrix} \gamma_{x1}(0) & \cdots & \gamma_{xn}(0) \\ \gamma_{x1}(\Delta x) & \cdots & \gamma_{xn}(\Delta x) \\ \vdots & & \vdots \\ \gamma_{x1}(j) & \cdots & \gamma_{xn}(j) \\ \vdots & & \vdots \\ \gamma_{x1}(L) & \cdots & \gamma_{xn}(L) \end{bmatrix}_{p\times n}, \gamma_i(x) = \frac{\mu_i(x)}{\sum_{k=1}^{n}\mu_k(x)},$$

where $\gamma_{xi}(x) = \dfrac{\partial\gamma_i(x)}{\partial x}$ and $\mu(x)$ is a Gaussian function. In the purpose of sustaining the distributed solution characteristics such as continuity, smoothness, and infinite differentiability, the function has been considered to be Gaussian.

$$\mu_i(x) = \exp\left(\frac{1}{2}\left(\frac{x-a_i}{\sigma_i}\right)^2\right), \qquad i = \{1, \cdots, n\} \tag{4}$$

where a_i is the mean and σ_i is the standard deviation of the i^{th} Gaussian function. These parameters a_i and σ_i can be computed as follows

$$a_i = (i-1)\frac{L}{n-1}, \qquad \sigma_i = \sigma = \alpha\frac{L}{n-1}, \quad \alpha{>}0.$$

The nonlinear state space representation is given as follows

$$\begin{cases} \dot{\xi}(t) = A\xi(t)u(t) + B(t), \\ y(t) = C\xi(t), \end{cases} \quad \text{where} \tag{5}$$

$$A = -\left(\Gamma^T\Gamma\right)^{-1}\Gamma^T\Gamma_x, \quad B(t) = \left(\Gamma^T\Gamma\right)^{-1}\Gamma^T S(t),$$
$$C = \Big[\gamma_1(L), ..., \gamma_n(L)\Big].$$

3. ADAPTIVE FEEDBACK-CONTROL DESIGN

In general, solar power plant models consider all field equipment acts the same for easier and simpler control design. For instance, the model presented in (1) has been widely used considering a homogeneous source term along the solar field. However, the solar irradiance and mirror efficiency can only be evaluated locally. Therefore, it is not reasonable assumption when we extrapolate these local measurements. For example, part of the pipe may not be receiving sunlight due to the clouds, which may effect the measurements locally. Also, dusty humid environment affects the mirrors optical efficiency.

Our goal is to design an adaptive controller to stabilize the tracking error of the closed-loop system. Fig. 2 presents the closed loop scheme of the system, which exhibits the asymptotic reference tracking regardless of the change in working conditions considering the source term inaccessibility.

As described in Elmetennani and Laleg-Kirati (2017), a nominal model of the system can be described as follows:

$$\begin{cases} \dot{\overline{\xi}}(t) = A\overline{\xi}(t)\overline{u}(t) + \overline{B}, \\ \overline{y}(t) = C\overline{\xi}(t), \end{cases} \quad \text{where} \tag{6}$$

$$\overline{B} = (\Gamma^T\Gamma)^{-1}\Gamma^T\overline{S} \quad \text{and} \quad \overline{S} = \frac{\overline{\nu_0}G}{\rho c A_s}\overline{I}\mathbf{1}_{px1}, \tag{7}$$

with $\overline{v_0} = 1$, $\overline{I} = 750W/m^2$, $\overline{\xi}$ is the state of the nominal model and $\overline{y}$ is the output of the nominal model, which describes the dynamics of the system to satisfy the nominal conditions.

3.1 Control Structure

The controller design for the tracking problem combines an inner loop feedback control with a model-free control to achieve the control objective performance. The tracking problem is divided into two parts

- Design a controller $\overline{u}$ with a nominal plant and a constant disturbance $\overline{S}$ such that
$$\lim_{t\to\infty}\overline{e}(t) = \lim_{t\to\infty}\overline{y}(t) - y^d(y) = 0, \tag{8}$$
- Design a control input u based on model-free structure that ensures
$$\lim_{t\to\infty}\underline{e}(t) = \lim_{t\to\infty} y(t) - \overline{y}(t) = 0, \tag{9}$$

where $y^d(t)$ is the desired temperature. The combination of both stabilizer guarantees the asymptotic convergence of the closed-loop system. The inner loop controller stabilizes the tracking error of the nominal system, while the outer loop stabilizes the tracking error between the nominal output and the real system output.

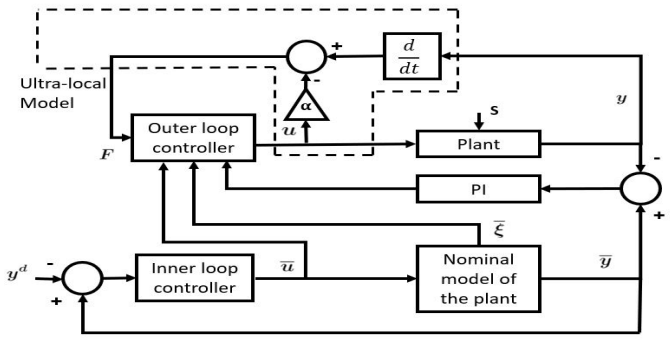

Fig. 2. Closed-loop system of the adaptive feedback control

3.2 Inner Loop Feedback Controller

The inner loop feedback controller is used for stabilizing the tracking error between the nominal system and the tracking reference. The tracking problem can be solved by choosing a proper control feedback function around the origin. As a result, the nominal system output is forced to track a preferable reference by the feedback control of the inner loop.

Proposition 1. The nominal system model (6) controlled by the following feedback control

$$\overline{u}(t) = \frac{-K_P\overline{e}(t) - K_I\int_0^t \overline{e}(\tau)d\tau + \dot{y}^d(t) - C\overline{B}}{CA\overline{\xi}(t)}, \quad (10)$$

is asymptotically stable which implies that the nominal system converges towards the reference.

Proof. To proof that proposition 1 holds for the nominal system (6), we consider the nominal tracking error as follows

$$\overline{e}(t) = C\overline{\xi}(t) - y^d(t). \quad (11)$$

The dynamics of the error is given as

$$\dot{\overline{e}}(t) = CA\overline{\xi}(t)\overline{u}(t) + C\overline{B} - \dot{y}^d(t). \quad (12)$$

Substituting the feedback controller (10) into (12), yields to the following equation

$$\dot{e}(t) + K_P e(t) + K_I\int_0^t e(\tau)d\tau = 0, \quad (13)$$

which implies the asymptotic convergence of the nominal system.

3.3 Outer Loop Model-Free Controller

The model-free control (MFC) is based on ultra-local model, which relates the input and the output and it is continuously updated as described in Fliess and Join (2009). This is useful when dealing with the uncertainties and unmodeled dynamics of the system to overcome these problems, especially for nonlinear system. In various applications the MFC was successfully applied Fliess and Join (2013, 2014); Abouaïssa et al. (2017); Choi et al. (2013); Villagra et al. (2009, 2012); Younes et al. (2016); Menhour et al. (2017); N'Doye et al. (2019). The following ultra-local model is used to find the adaptive control input

$$\dot{y}(t) = F(t) + \alpha u(t), \quad (14)$$

where F represents the effects of unmodeled dynamics and disturbances and α is chosen such that αu and $\dot{y}$ are of the same order of magnitude. We propose an intelligent proportional-integral (i-PI) control input u to guarantee the stability of the tracking error for the outer loop system. The control input u can be written as

$$u(t)=\frac{1}{\alpha}\Big[-F(t)+CA\dot{\overline{\xi}}(t)\overline{u}(t)+C\overline{B}+K_P\underline{e}(t)+K_I\int_0^t\underline{e}(\tau)d\tau\Big], \quad (15)$$

where $F(t)$ is continuously updated using the information from the control input u and the controlled output y as follows

$$F(t) = \hat{\dot{y}}(t) - \alpha u(t), \quad (16)$$

where $\hat{\dot{y}}(t)$ is updated via a receding horizon algebraic estimator Zehetner et al. (2007).

$$\hat{\dot{y}}(t) = \int_0^{t_a} \frac{180\tau^2 - 192\tau t_a + 36{t_a}^2}{{t_a}^4} y(t - t_a)d\tau, \quad (17)$$

such that t_a is the receding horizon window width. Thereafter, substituting (10) and (16) into (15) yields

$$-\hat{\dot{y}} + \dot{y}^d - K_P\overline{e}(t) - K_I\int_0^t \overline{e}(\tau)d\tau + K_P\underline{e}(t) + K_I\int_0^t \underline{e}(\tau)d\tau = 0. \quad (18)$$

Adding and subtracting $\dot{y}$ gives

$$\dot{y}^d - \dot{y} - K_P\overline{e}(t) - K_I\int_0^t \overline{e}(\tau)d\tau + K_P\underline{e}(t) + K_I\int_0^t \underline{e}(\tau)d\tau = \hat{\dot{y}} - \dot{y}. \quad (19)$$

Subsequently, with a good estimation of $F(t)$ using $\hat{\dot{y}}(t)$ computed from (17) leads to $\hat{\dot{y}} - \dot{y} \simeq 0$. Furthermore, since $\underline{e}(t) - \overline{e}(t) = y^d(t) - y(t)$ which can be defined as the error of the global system $e(t) = y^d(t) - y(t)$. Then, equation (19) become as follows

$$\dot{e}(t) + K_P e(t) + K_I\int_0^t e(\tau)d\tau = 0, \quad (20)$$

that ensures asymptotic convergence of the desired reference for the closed-loop system. Compared to the practical stability convergence proposed in Elmetennani and Laleg-Kirati (2017), here we achieve asymptotic convergence and accurate tracking.

Table 2. RMSE Performance Comparison.

Solar irradiance profiles	Smooth	Varying	Abrupt
i-P controller	1.24	1.27	1.28
i-PI controller	1.14	1.17	1.18
Improvement	8.06%	7.87%	7.81%

4. RESULTS AND DISCUSSION

In this section, the controller performance has been evaluated numerically using the ACUREX field parameters. The evaluation was based on three different solar irraidance profiles. First, the controller behaviour has been evaluated consider ideal working conditions using smooth solar irradiance profile presented in Fig.3 a). The second test was carried out with some rapid changes in the solar irradiance using a varying profile in Fig. 4 a). The third test an extreme working conditions have been considered using the abrupt solar irradiance profile in Fig. 5 a).

In these tests, physical limitations of the actuator have been considered to ensure that the flow rate is in the

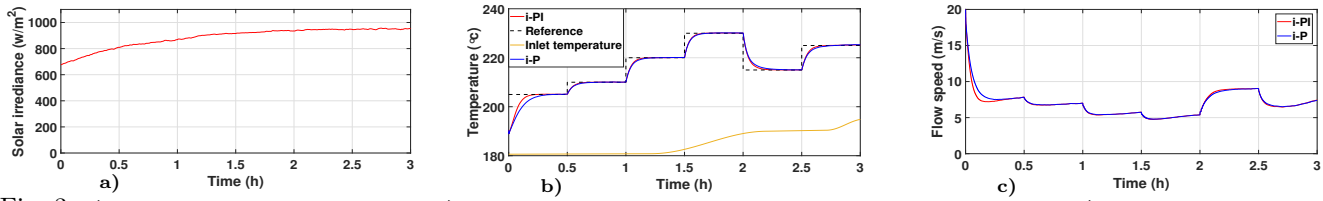

Fig. 3. **a)** Smooth solar irradiance profile; **b)** Closed-loop tracking responses using i-PI and i-P controllers; **c)** Control input.

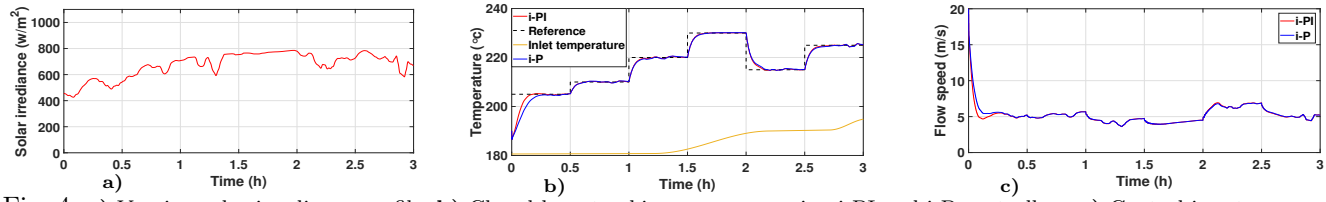

Fig. 4. **a)** Varying solar irradiance profile; **b)** Closed-loop tracking responses using i-PI and i-P controllers; **c)** Control input.

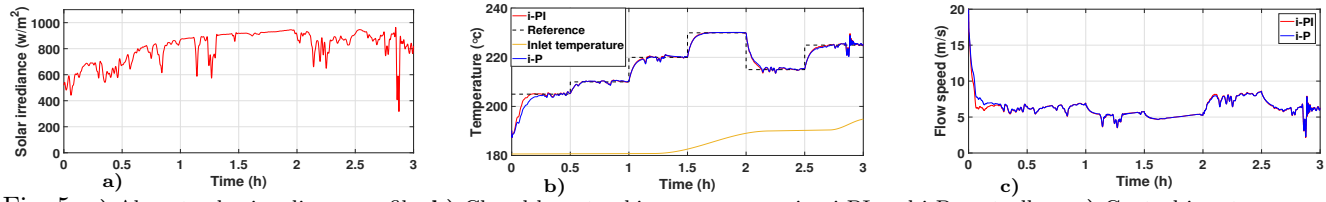

Fig. 5. **a)** Abrupt solar irradiance profile; **b)** Closed-loop tracking responses using i-PI and i-P controllers; **c)** Control input.

admissible range. The closed loop time response of the proposed controller is managed through tuning the design parameters K_P and K_I. In Elmetennani and Laleg-Kirati (2017) an i-P was introduced with $K_P = 0.005$. For the proposed i-PI multiple tests showed that increasing K_P more than 0.007 and K_I more than 0.005 causes oscillation and instability of the system due to the physical limitation of the actuator. Although, decreasing K_P results in slower transient time and decreasing K_I increases the tracking error. Therefore, for these tests to obtain the desirable performance in terms of convergence time and tracking error, we chose K_P and K_I to be 0.007 and 0.005, respectively. Table 2 shows the RMSE performance of the proposed i-PI controller verses i-P controller introduced in Elmetennani and Laleg-Kirati (2017).

The obtained results of the three different tests using smooth, varying and abrupt solar irradiance profile are presented in Fig. 3, 4 and 5 respectively. From the closed loop responses it can be observed that the outlet temperature using i-PI controller is accurately tracking the reference level and faster than i-P controller. The gained improvement in the tracking error is due to the asymptotic stability and additional integration term compared with the i-P that had bounded convergence. In addition, the control input is adapting to the different levels of variations in the external working conditions and show reasonable behavior, which maintain the closed loop stability within the admissible range of the flow rate.

- Solar driven MD Performance: As shown in Table 2, the objective of the proposed i-PI controller improved the energy production. This improvement benefits the water production by combining the solar driven MD process as illustrated in Fig. 1.

The Direct Contact Membrane Distillation model introduced in Karam and Laleg-Kirati (2016) is used to obtain the distillated water flux by entering the outlet temperature obtained from the solar collector using both i-P and i-PI controllers. The root mean square error (RMSE) evaluates the performance of the water flux using i-P and i-PI controllers on different and overall simulation time intervals. Table 3 shows the performance enhancements of the water production by considering three solar irradiance profiles. Finally, the performance of the integrated solar DCMD improved by 12% in the first time half hour interval and 5% in the overall time period.

5. CONCLUSION

In this work, an adaptive control design has been proposed for concentrated distributed solar collector. The proposed controller combines an inner loop feedback control and a model-free control to force the outlet temperature to track the reference level. Furthermore, the proposed adaptive controller has been tested numerically under three different working conditions to achieve satisfactory tracking performance results. Finally, the proposed adaptive control improves the water production in the combined solar-power desalination.

REFERENCES

Abouaïssa, H., Fliess, M., and Join, C. (2017). On ramp metering: Towards a better understanding of ALINEA via model-free control. *Int. J. Control*, 90, 1018–1026.

Bendevis, P., Karam, A., and Laleg-Kirati, T.M. (2019). Optimal model-free control of solar thermal membrane distillation system. *Computers Chemical Engineering*, 106622.

Camacho, E., Rubio, F., Berenguel, M., and Valenzuela, L. (2007a). A survey on control schemes for distributed solar collector fields. Part II: Advanced control approaches. *Solar Energy*, 81(10), 1252–1272.

Camacho, F.E. and Berenguel, M. (1997). Robust adaptive model predictive control of a solar plant with bounded uncertainties. *International Journal of Adaptive Control and Signal Processing*, 11(4), 311–325.

Table 3. RMSE: Performances Enhancements of the Water Production

Interval of time (minutes)	$[0, 30]$min	$[30, 60]$min	$[60, 90]$min	$[90, 120]$min	$[120, 150]$min	$[150, 180]$min	$[0, 180]$min
Smooth	10.36%	1.17%	1.89%	1.32%	2.68%	2.82%	4.64%
Time-varying	12.84%	0.68%	1.63%	0.93%	2.04%	1.94%	5.43%
Abrupt	11.76%	1.01%	2.38%	1.38%	2.17%	3.09%	5.18%

Camacho, F.E., M. Berenguel, M.M., and Rubio, F.R.F.R. (1997). *Advanced Control of Solar Plants*. Springer.

Camacho, F.E., Rubio, R.F., Berenguel, M., and Valenzuela, L. (2007b). A survey on control schemes for distributed solar collector fields. Part I: Modeling and basic control approaches. *Solar Energy*, 81, 1240–1251.

Camacho, F.E., Rubio, R.F., and Hughes, M.F. (1992). Self-tuning control of a solar power plant with a distributed collector field. *IEEE Control Systems*, 12(2), 72–78.

Carotenuto, L., Cava, L.M., and Raiconi, G. (2007). Regulator design for the bilinear distributed-parameter model of a solar-power plant. *International Journal of Systems Science*.

Choi, S., Andréa-Novel, B., Fliess, M., Mounier, H., and Villagra, J. (2013). Multivariable decoupled longitudinal and lateral vehicle control: A model-free design. In *Conf. on Dec. and Cont.*, 2834–2839. Florence, Italy.

Cirre, C.M., Berenguel, M., Valenzuela, L., and Camacho, E.F. (2007). Feedback linearization control for a distributed solar collector field. *Control Engineering Practice*, 15(12), 1533–1544.

Elmetennani, S. and Laleg-Kirati, T.M. (2016). Bilinear reduced order approximate model of parabolic distributed solar collectors. *Solar Energy*, 131, 71–80.

Elmetennani, S. and Laleg-Kirati, T.M. (2017). Bilinear approximate model-based robust Lyapunov control for parabolic distributed collectors. *IEEE Transactions on Control Systems Technology*, 25(5), 1848–1855.

Farkas, I. and Vajk, I. (2002). Internal model-based controller for a solar plant. *IFAC Proceedings Volumes*, 35(1), 49–54.

Fliess, M. and Join, C. (2013). Model-free control. *Int. J. of Control*, 86, 2228–2252.

Fliess, M. and Join, C. (2014). Stability margins and model-free control: A first look. In *Eur. Contr. Conf.* Strasbourg, France.

Fliess, M. and Join, C. (2009). Model-free control and intelligent pid controllers: towards a possible trivialization of nonlinear control? *IFAC Proceedings Volumes*, 42(10), 1531–1550.

Gallego, J.A. and Camacho, F.E. (2012). Adaptive state-space model predictive control of a parabolic-trough field. *Control Engineering Practice*, 20(9), 904–911.

Guo, X., Albalawi, F., and Laleg-Kirati, T.M. (2019). Model predictive control paradigms for direct contact membrane desalination modeled by differential algebraic equations. In *American Control Conference (ACC)*, 5595–5601.

Gálvez, J.B., García-Rodríguez, L., and Martín-Mateos, I. (2009). Seawater desalination by an innovative solar-powered membrane distillation system: the MEDESOL project. *Desalination*, 246(1), 567 – 576.

Henriques, J., Cardoso, A., and Dourado, A. (1999). Supervision and c-means clustering of PID controllers for a solar power plant. *International Journal of Approximate Reasoning*, 22(1-2), 73–91.

Igreja, J., Lemos, J., and Silva, R. (2014). Adaptive receding horizon control of a distributed collector solar field. In *44th IEEE Conf. on Dec. and Cont.*, 1282–1287.

João, L., Neves-Silva, R., and Igreja, M.J. (2014). *Adaptive control of solar energy collector systems advances in industrial control*. Springer.

Johansen, T.A. and Storaa, C. (2002). Energy-based control of a distributed solar collector field. *Automatica*, 38(7), 1191–1199.

Karam, A.M. and Laleg-Kirati, T.M. (2016). Electrical equivalent thermal network for direct contact membrane distillation modeling and analysis. *Journal of Process Control*, 47, 87 – 97.

Menhour, L., Andréa-Novel, B., M. Fliess, D.G., and Mounier, H. (2017). An efficient model-free setting for longitudinal and lateral vehicle control. validation through the interconnected pro-SiVIC/RTMaps prototyping platform. *IEEE Trans. Intel. Transport. Syst.*

N'Doye, I., Asiri, S., Aloufi, A., and Laleg-Kirati, T.M. (2019). Intelligent proportional-integral-derivative control-based modulating functions for laser beam pointing and stabilization. *IEEE Transactions on Control Systems Technology*, 1–8.

Orbach, A., Rorres, C., and Fischl, R. (1981). Optimal control of a solar collector loop using a distributed-lumped model. *Automatica*, 17(3), 535–539.

Pin, G., Falchetta, M., and Fenu, G. (2008). Adaptive time-warped control of molten salt distributed collector solar fields. *Control Engineering Practice*, 16(7), 813–823.

Rorres, C., R., A.O., and Fischl (1980). Optimal and suboptimal control policies for a solar collector system. *IEEE Transactions on Automatic Control*, 25(6), 1085–1091.

Silva, N.R., Lemos, M.J., and Rato, M.L. (2003a). Variable sampling adaptive control of a distributed collector solar field. *IEEE Transactions on Control Systems Technology*, 11(5), 765–772.

Silva, R., Rato, L., and Lemos, J. (2003b). Time scaling internal state predictive control of a solar plant. *Control Engineering Practice*, 11(12), 1459–1467.

Villagra, J., , and Herrero-Pérez, D. (2012). A comparison of control techniques for robust docking maneuvers for an AVG. *IEEE Trans. Control Syst. Technol.*, 20, 1116–1123.

Villagra, J., Andréa-Novel, B., Choi, S., Fliess, M., and Mounier, H. (2009). Robust stop-and-go control strategy: An algebraic approach for nonlinear estimation and control. *Int. J. Vehicle Auto. Syst.*, 7, 270–291.

Younes, Y.A., Drak, A., Noura, H., Rabhi, A., and Hajjaji, A.E. (2016). Robust model-free control applied to a quadrotor UAV. *J. Intell. Robot Syst.*, 84, 37–52.

Zehetner, J., Reger, J., and Horn, M. (2007). A derivative estimation toolbox based on algebraic methods - theory and practice. In *IEEE Int. Conf. on Cont. Appl.*, 331–336.